Signal dependence of the phase-generated carrier method

Kuang Wu
Zhang Min
Yanbiao Liao
Tsinghua University
Department of Electronic Engineering
Beijing, China, 100084
E-mail: kuangwu@tsinghua.org.cn

Abstract. The phase-generated carrier (PGC) is the best-known signal-processing method for an optical fiber interferometer, and has been widely adopted for experimental systems such as hydrophones and optical fiber current sensors. It has many advantages, such as high resolution and passive sensor structure, and has been used for more than 20 years. In this paper, the signal dependence of the PGC is reported for the first time. Our results imply, in view of the highpass filter that is needed to suppress the temperature fluctuation of the interferometer, that the application of the PGC method is inappropriate for the measurement of low-frequency but sharp-rising-edge signals, such as seismic signals, whose frequency extends down to ~1 Hz and whose rising edge is very sharp. In such a case, the signal dependence will cause fatal errors. Experimental and simulation results are provided to describe the defects of this method. An analysis of the restrictions on the use of the PGC method is also provided. [DOI: 10.1117/1.2799518]

Subject terms: fiber optic interferometer; PGC; initial phase; highpass filter.

Paper 060163R received May 20, 2006; revised manuscript received Apr. 21, 2007; accepted for publication Apr. 30, 2007; published online Oct. 24, 2007.

1 Introduction

The fiber optic interferometer has been used as a vibration sensor for more than 20 years. With its high sensitivity and large dynamic range, it can give much higher performance than conventional electronic transducers. However, the high performance comes at the price of a more complicated demodulation method. The output signal of a sensor based on a fiber optic interferometer is phase- rather than amplitude-modulated, and so less straightforward to demodulate.

In order to get the detected signal from the output of the interferometer, many methods of signal processing have been proposed. Among those methods, the phase-generated carrier (PGC) is the best-known one and has been widely adopted for experimental systems such as hydrophones and optical fiber current sensors.[1–5] In addition to sensors based on interferometers, the PGC can be used as the demodulation system for sensors based on the fiber Bragg grating (FBG).[6,7]

Figure 1 shows the principle of the PGC method. Basically the interferometric signal is a cosine function; its phase cannot be recovered by a simple arccosine process, because it is not a linear signal. The PGC is used to produce two other functions by additional phase modulation. With these new functions, the phase of interferometer can be recovered directly.

2 Analysis

The output signal of an optical fiber interferometer can be represented as

$$I = A + B\cos\phi. \tag{1}$$

It is labeled as **1** in Fig. 1. Here A is the dc component, which is determined entirely by the optical power and is independent of the detected signal; B represents the interferometric visibility, which is determined by the optical power and the polarization state of the light beams involving interference; and ϕ is the phase difference between the two arms of the interferometer, which can be caused either by the variation of optical length or by variation of the wavelength of the light source.[1,2] Here ϕ can be expressed as

$$\phi = \frac{2\pi}{\lambda} nl, \tag{2}$$

where λ is wavelength of the light source, and nl is the interferometer's optical length, which is the product of the refractive index n and the length difference Z of the two arms of the fiber interferometer.

In the PGC method, ϕ can be written as

$$\phi = C\cos\omega_c t + \phi_s, \tag{3}$$

where $C\cos\omega_c t$ is the carrier signal, which is added by the PGC modulator, C and ω_c being its amplitude and frequency. The amplitude C depends on the path difference of the interferometer and the wavelength modulation depth of the laser source. The term ϕ_s is the interferometer phase variation caused by the detected signal.

As shown in Fig. 1, the output of the two mixers and the two lowpass filters can be represented as

$$S_1 = BJ_2(C)\cos\phi_s, \tag{4}$$

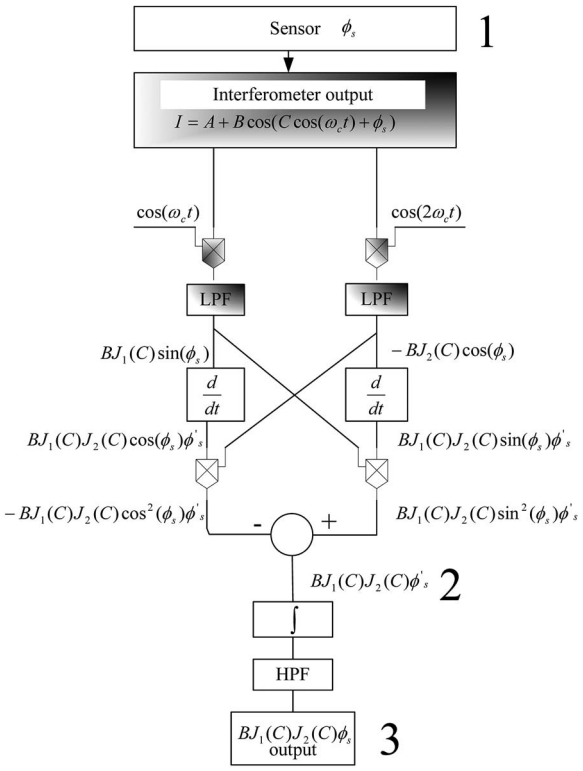

Fig. 1 Schematic diagram of PGC method.

$$T_1 = BJ_1(C)\sin\phi_s, \tag{5}$$

where $J_1(C)$ and $J_2(C)$ are first- and second-order Bessel functions with the argument C, and S_1 and T_1 are two orthogonal signals, which extract from the original interferometric signal carrier sufficient information to resolve the signal being detected.

After differentiation, cross-multiplication, and subtraction, the signal at the input to the integrator can be represented as

$$B^2J_1(C)J_2(C)\phi'_s \tag{6}$$

and is labeled as **2** in Fig. 1. After the integration, the signal to be detected can be recovered as

$$B^2J_1(C)J_2(C)\phi_s. \tag{7}$$

The PGC method has been widely used for demodulation of high-frequency signals, such as that of a hydrophone. When the method is applied in high-frequency measurement, there is no signal dependence, and that independence is a fundamental requirement of such a system. However, when it is used for low-frequency measurement, as with seismic sensors, a signal dependence problem arises.

In order to get Eq. (7), the lower limit of integration should be zero. That condition can be satisfied if a signal has the form of a pure sine wave. But this is not the common case. When there is a phase shift of the sine wave, as in $\sin(\omega_s t+\phi_0)$, with ϕ_0 being the initial phase of the measured signal, Eq. (6) can be represented as

$$B^2J_1(C)J_2(C)\omega_s\cos(\omega_s t + \phi_0). \tag{8}$$

Then Eq. (7) should be rewritten as

$$\begin{aligned}\text{output} &= \int_0^{t_1} B^2J_1(C)J_2(C)\omega_s\cos(\omega_s\tau + \phi_0)\,\mathrm{d}\tau \\ &= B^2J_1(C)J_2(C)\sin(\omega_s t + \phi_0)\big|_{\tau=0}^{\tau=t} \\ &= B^2J_1(C)J_2(C)\sin(\omega_s t + \phi_0) - B^2J_1(C)J_2(C)\sin\phi_0.\end{aligned} \tag{9}$$

So the recovered signal will be composed of the detected signal and an additional dc component, which is determined by the initial phase of the detected signal. When the sensors are tested in a laboratory environment, the signal source is always chosen to be sinusoidal, so the condition can always be satisfied. When the sensors are used in the field, a problem arises immediately. The step value caused by the initial phase acts as noise with a large and variable frequency range, which cannot be filtered by the following highpass filter. There are different cases, which are presented in the next section.

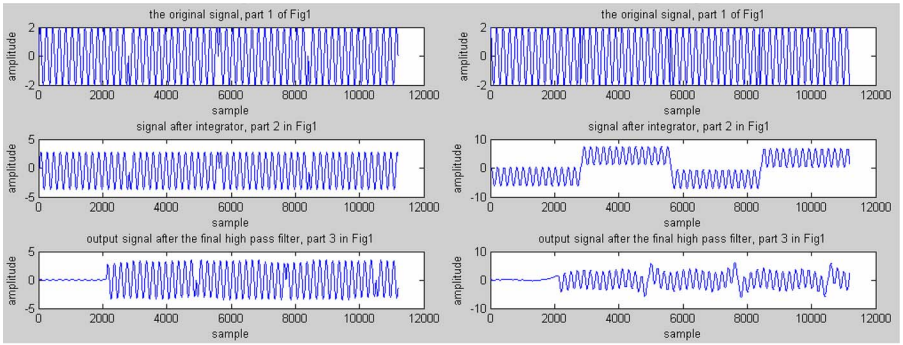

(a) Sine signal (b) Cosine signal

Fig. 2 Simulation results for sine and cosine signals with constant envelope. Top: Stimulus signal labeled 1 in Fig. 1; middle: signal labeled **2** in Fig. 1; bottom: output signal labeled **3** in Fig. 1.

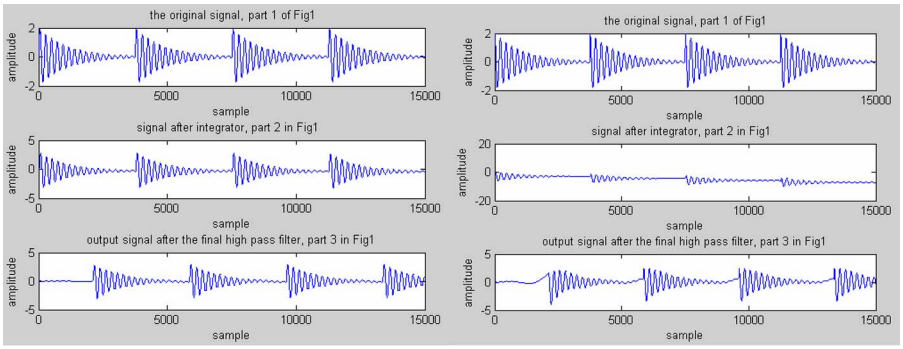

(a) Sine signal (b) Cosine signal

Fig. 3 Simulation result for exponential burst packet with frequency much larger than the burst frequency. Top: stimulus signal labeled **1** in Fig. 1; middle: signal labeled **2** in Fig. 1; bottom: output signal labeled **3** in Fig. 1.

3 Simulations and Experiments

In order to prove the preceding analysis, many different signals are considered in simulation. The simulation is based on Eqs. (1) to (7), with the carrier frequency 11.2 kHz and the sampling rate 112 kHz. The signals labeled **1**, **2**, **3** in Fig. 1 have been plotted in Figs. 2–4, respectively.

1. Signals with constant envelope. This is the laboratory case, and we use a passive detection system:

a. Sine signal with phase steps $\Delta\phi=\pi$ at each point of discontinuity:

$$\phi_s=\begin{cases}\sin\omega_s t, & 0<t\le T,\\ \sin(\omega_s t+\pi), & T<t\le 2T,\\ \sin\omega_s t, & 2T<t\le 3T,\\ \sin(\omega_s t+\pi), & 3T<t\le 4T.\end{cases} \tag{10a}$$

b. Cosine signal with phase steps $\Delta\phi=\pi$ at each point of discontinuity:

$$\phi_s=\begin{cases}\cos\omega_s t, & 0<t\le T,\\ \cos(\omega_s t+\pi), & T<t\le 2T,\\ \cos\omega_s t, & 2T<t\le 3T,\\ \cos(\omega_s t+\pi), & 3T<t\le 4T,\end{cases} \tag{10b}$$

Here T is the time slot which the measured signal phase (*not* the interferometric phase) change is π. The result is shown Fig. 2.

2. Signals with exponential burst packets, with the burst frequency much lower than that of the detected signal.

a. Sine signal with phase steps $\Delta\phi=\pi$ at each point of discontinuity:

$$\phi_s=\begin{cases}\exp(-\alpha t)\sin\omega_s t, & 0<t\le T,\\ \exp[-\alpha(t-T)]\sin(\omega_s t+\pi), & T<t\le 2T,\\ \exp[-\alpha(t-2T)]\sin\omega_s t, & 2T<t\le 3T,\\ \exp[-\alpha(t-3T)]\sin(\omega_s t+\pi), & 3T<t\le 4T.\end{cases} \tag{11a}$$

b. Cosine signal with phase steps $\Delta\phi=\pi$ at each point of discontinuity:

$$\phi_s=\begin{cases}\exp(-\alpha t)\cos\omega_s t, & 0<t\le T,\\ \exp[-\alpha(t-T)]\cos(\omega_s t+\pi), & T<t\le 2T,\\ \exp[-\alpha(t-2T)]\cos\omega_s t, & 2T<t\le 3T,\\ \exp[-\alpha(t-3T)]\cos(\omega_s t+\pi), & 3T<t\le 4T.\end{cases} \tag{11b}$$

The result is shown in Fig. 3.

3. Same as signal 2, but the frequency of the measured signal is of the same order as the burst frequency. This case is very similar to that of the field signal in seismic measurement, which has an air-gun time slot of the same order as the period of the detected low-frequency signal. The result is shown in Fig. 4.

For comparison with the simulation, an experiment with the setup shown in Fig. 5 is reported. This experiment was made within a large swimming pool. The parameters (data sampling rate, modulation depth C) in the experimental system are the same as those in the simulation.

Figure 6 shows some results obtained on an oscilloscope. There are two traces in each part: the upper one is from the fiber optic sensor, and the lower one is a piezoelectric transducer from (PZT) sensor as a reference. In Fig. 6(a) the stimulus signal is from a loudspeaker with pure harmonic sound. In Fig. 6(b) the stimulus signal was made by clicking one piece of iron against another; the signal in this case has very sharp rising edge. According to this figure, it is clear that when the signal is weak, the fiber optic sensor can detect it when it is missed by the PZT. This is due to the high sensitivity of the optical fiber interferometer. When the signal has a sharp change, the signal will

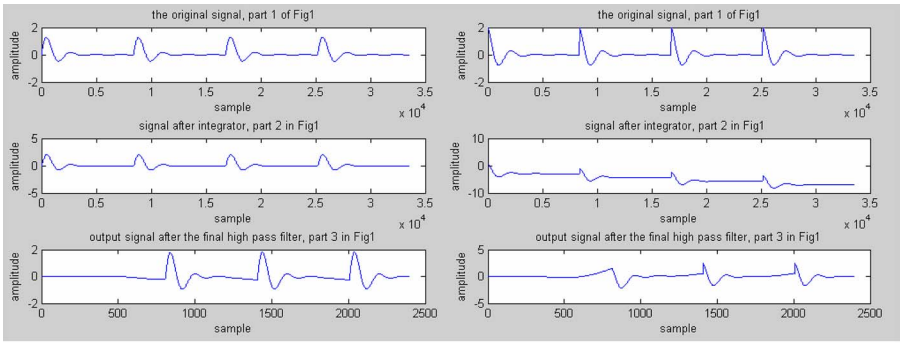

(a) Sine signal (b) Cosine signal

Fig. 4 Exponential burst packet with burst frequency of the same order as the signal. Top: stimulus signal labeled **1** in Fig. 1; middle: signal labeled **2** in Fig. 1; bottom: output signal labeled **3** in Fig. 1.

clearly distort, but the sensor based on a PZT can work properly in this case, due to the PZT's linearity.

4 Discussion

Because the initial phase of the field signal will not be zero in all cases, distortion of the recovered signal will arise. The nonzero initial phase is introduced mainly in three ways:

1. *Nonzero initial value*. Using Fourier transformation, any signal can be decomposed into sine components; when the sine components have zero initial phase, they will have zero initial value. When the first value sampled by the sensor is nonzero, it is impossible to decompose the signal into sine components with zero initial phase; it must have many sine components with different frequency, amplitude, and especially phase. In our experiment, the sound generated by collision between pieces of iron is found to have nonzero initial phase, and a sharp jump appears in Fig. 6(b). The sound generated by collision between pieces of iron and pieces of plastic is found to be better in this respect than for iron with iron.
2. *The acceleration of the measured system*. If the sensor under test is accelerated, it will introduce a signal with nonzero initial value, because acceleration is proportional to force when mass is constant. Though the vibration needs time to propagate, the force does not. Thus a sudden force can introduce a sudden acceleration, which can be converted to a signal with nonzero initial value. The results of the experiment made in the swimming pool provide a proof of this conclusion.
3. *The acquisition time of a digital PGC system*. When digitization is performed, the time slot between samples may cause the zero initial value to be lost. A higher sampling rate will result in shorter timing slots, which will make the front edge of the measured signal steeper. When the sampling rate is not high enough, the time slot will be converted to a nonzero initial phase, for which the relationship is $\phi_0 = 2\pi T_{\text{sample}}/T_{\text{signal}}$.

As mentioned in the analysis section, the step functions among signals past the integrator can be treated as a noise with wide and variable frequency. A highpass filter as in Fig. 1 is often used to remove the shift arising from temperature changes and other very slow phenomena. When the detected signal has high enough frequencies to be far away from the step frequency, then the step function will be filtered along with the slow shifts. That is the case with hydrophone signals, of which the frequency range is always higher than 1 kHz. But when the PGC system is used for a seismic sensor, the condition is very different: A signal stimulated by an air gun (the signal source in seismic measurement) and then reflected by the earth contains very low-frequency elements, down to 3 Hz, and the initial value is almost random. In this case highpass filtering cannot distinguish signal and noise. According to signal-processing theory, a highpass filter with cutoff frequency much lower than the sampling rate will act as a differentiator, so that a step function is changed to an impulse function by the filter.

The problem of initial phases is inherent in the PGC method represented in Fig. 1. Recently a modified method has been proposed with the objective of simplifying the PGC.[8] The integrator is not required in the modified method, so the problem of signal dependence disappears. However, the scheme shown in Fig. 1 is preferred for most systems, because there are some difficulties in making the modified PGC method satisfy the strict requirement of

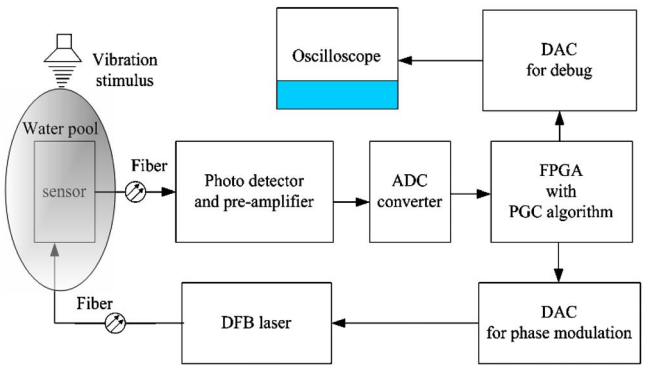

Fig. 5 Experimental setup.

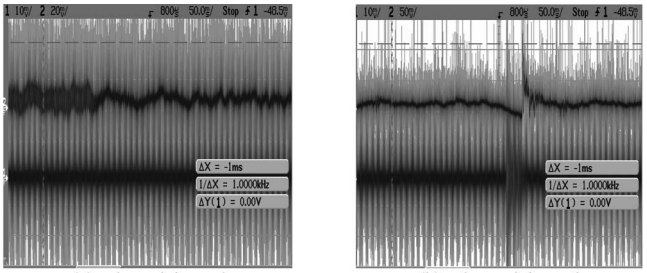

(a) slow rising edge (b) sharp rising edge

Fig. 6 Oscilloscope trace of measured sensor signals. Top: output from fiber optic interferometer with PGC; bottom: output from PZT sensor as a reference.

modulation depth. For the calculation of the arctangent, a finger counter is needed, and its accuracy cannot be well guaranteed.

The method in Fig. 1 avoids those problems in the modified PGC method, but the problem of signal dependence restricts its application. Either scheme may be appropriate, depending on details.

First the signal parameters, especially the required frequency range and signal continuity, should be examined carefully. Optimization of these parameters may ensure that the distortion of the leading part of the signal, which is an ultimate limitation of such a system, is acceptable. If the frequency range is suitable, the scheme in Fig. 1 is preferable.

Alternatively, when many wave packets arrive at the sensor with a burst frequency of the same order of magnitude as the signal frequency, the scheme in Fig. 1 is not suitable, because the leading part of signal in positive detection is important for synchronization of the wave packet. Then the modified method[8] should be used instead, with some degradation of accuracy.

5 Conclusion

In this paper, signal dependence of the PGC method has been reported for the first time. Simulation and experimental results are given here as a reference for those fiber optic interferometer systems using, PGC. The designers of different systems based on fiber optical interferometers can benefit from these considerations.

Acknowledgment

The authors would like to acknowledge financial support from Petrotech Services, CNOOC (China National Offshore Oil Corp.).

References

1. A. Dandridge, A. B. Tveten, and T. G. Giallorenzi, "Homodyne demodulation scheme for fiber optic sensors using phase generated carrier," *IEEE J. Quantum Electron.* **QE-18**(10), 1647–1653 (1982).
2. A. Dandridge and A. D. Kersey, "Signal processing for optical fiber sensors," in *Fiber Optic Sensors II*, *Proc. SPIE* **798**, 158–165 (1987).
3. C. K. Kirkendall and A. Dandridge, "Overview of high performance fibre-optic sensing," *J. Phys. D* **37**, R197–R216 (2004).
4. G. A. Cranch, P. J. Nash, and C. K. Kirkendall, "Large-scale remotely interrogated arrays of fiber-optic interferometric sensors for underwater acoustic applications," *IEEE Sens. J.* **3**(1), 19–30 (2003).
5. W.-W. Lin, "Fiber-optic current sensor," *Opt. Eng.* **42** 896–897 (2003).
6. G. A. Cranch, G. M. H. Flockhart, and C. K. Kirkendall, "Efficient Bragg grating and fiber Fabry-Perot sensor multiplexing scheme using a broadband pulsed mode-locked laser," *J. Lightwave Technol.* **23**(11), 3798–3807 (2005).
7. T. A. Berkoff and A. D. Kersey, "Experimental demonstration of a fiber Bragg grating accelerometer," *IEEE Photonics Technol. Lett.* **8**(12), 1677–1679 (1996).
8. J. Bush, A. Cekorich, and C. Kirkendall, "Multi-channel interferometer demodulator," in *Third Pacific Northwest Fiber Optic Sensor Workshop*, *Proc. SPIE* **3180**, 19–29 (1997)..